Electron capture in GaAs quantum wells via electron-electron and optic phonon scattering

K. Kálna and M. Moško
Institute of Electrical Engineering, Slovak Academy of Sciences, Dúbravská cesta 9, Sk-842 39 Bratislava, Slovakia

F. M. Peeters
Department of Physics, University of Antwerp (UIA), Universiteitsplein 1, B-2610 Antwerpen-Wilrijk, Belgium

(Received 14 June 1995; accepted for publication 17 October 1995)

Electron capture times in a quantum well (QW) structure with finite electron density are calculated for electron-electron (e-e) and electron-polar optic phonon (e-pop) scattering. We find that the capture time oscillates as function of the QW width for both processes with the same period, but with very different amplitudes. For an electron density of 10^{11} cm^{-2} the e-e capture time is 10^1-10^3 times larger than the e-pop capture time except for QW widths near the resonance minima, where it is only $2-3$ times larger. With increasing density the e-e capture time decreases and near the resonance becomes smaller than the e-pop capture time. Our e-e capture times are three orders larger than the results of Blom *et al.* [Appl. Phys. Lett. **62**, 1490 (1993)]. The role of the e-e capture in QW lasers is therefore readdressed. © *1996 American Institute of Physics.* [S0003-6951(95)02752-8]

The electron capture in a quantum well plays an important role in optimizing the performance of separate confinement heterostructure quantum well (SCHQW) lasers. Quantum calculations[1] of polar optic phonon (pop) emission induced capture in GaAs QW predicted oscillations of the capture time versus the QW width, which have been observed.[2] The minima of the oscillations provide the optimum well and barrier width for an optimized capture. At high electron densities the electron-electron (e-e) scattering induced capture is expected to be important. Blom *et al.*[3] predicted that the e-e capture time in a GaAs QW with electron density of 10^{11} cm^{-2} oscillates with nearly the same amplitude and period as the e-pop capture time. Away from the oscillation minima the e-pop capture was weak and the e-e capture was expected to increase the threshold current in the SCHQW laser via excess carrier heating in the QW.[3]

In this letter the e-e and e-pop scattering induced capture times are recalculated for the same SCHQW as in Ref. 3. We find that for an electron density of 10^{11} cm^{-2} the e-e capture time is 10^1-10^3 times larger except for QW widths near the resonance minima, where it is only $2-3$ times larger. For densities above $\sim 5\times 10^{11}$ cm^{-2} the resonant e-e capture time is smaller than the e-pop capture time. This optimizes the capture. The e-e capture is found to be too weak to cause an excess carrier heating which is in contrast to Ref. 3.

We analyze the $Al_xGa_{1-x}As/GaAs/Al_xGa_{1-x}As$ QW with 500 Å $Al_xGa_{1-x}As$ barriers, embedded between two thick AlAs layers. When two electrons in subbands i,j with wave vectors $\mathbf{k}$ and $\mathbf{k}_0$ are scattered to subbands m,n with wave vectors $\mathbf{k}'$ and $\mathbf{k}_0'$, the e-e scattering rate of an electron with wave vector $\mathbf{k}$ from subband i to subband m reads[4]

$$\lambda_{im}(\mathbf{k})=\frac{1}{N_S A}\sum_{j,n,\mathbf{k}_0} f_j(\mathbf{k}_0)\lambda_{ijmn}(g), \tag{1}$$

where $g=|\mathbf{k}-\mathbf{k}_0|$,

$$\lambda_{ijmn}(g)=\frac{N_S m^* e^4}{16\pi\hbar^3\kappa^2}\int_0^{2\pi} d\theta \frac{F_{ijmn}^2(q)}{q^2\epsilon^2(q)}, \tag{2}$$

$$q=\frac{1}{2}\left[2g^2+\frac{4m^*}{\hbar^2}E_S-2g\left(g^2+\frac{4m^*}{\hbar^2}E_S\right)^{1/2}\cos\theta\right]^{1/2}, \tag{3}$$

$$F_{ijmn}(q)=\int_{-\infty}^{\infty}dz\int_{-\infty}^{\infty}dz_0\chi_i(z)\chi_j(z_0)\times e^{-q|z-z_0|}\chi_m(z)\chi_n(z_0). \tag{4}$$

$E_S=E_i+E_j-E_m-E_n$, the summation over $\mathbf{k}_0$ includes both spin orientations, m^* is the electron effective mass in GaAs, κ the static permittivity, A the normalization area, E_j the subband energy and $f_j(\mathbf{k}_0)$ the electron distribution in subband j. Wave functions χ_i are obtained assuming the x-dependent, flat Γ-band with parabolic energy dispersion, interpolated[5] between the GaAs and AlAs. To deal with the 0.3-eV QW[3] we take $x=0.305$. The e-e capture time $\tau_{e-e}=\Sigma_{i,\mathbf{k}}f_i(\mathbf{k})/\Sigma_{i,\mathbf{k},m}f_i(\mathbf{k})\lambda_{i,m}(\mathbf{k})$, where the summation over i (m) includes the subbands above (below) the AlGaAs barrier, and summation over j,n in Eq. (1) involves the subbands below the AlGaAs barrier. $f_j(\mathbf{k}_0)$ is the Fermi function taken at temperature 8 K and for an electron density $N_S=10^{11}$ cm^{-2}. $\epsilon(q)=1+(q_S/q)F_{1111}(q)f_1(\mathbf{k}_0=0)$ is the static screening function due to the electrons in the lowest subband,[4] where $q_S=e^2m^*/(2\pi\kappa\hbar^2)$.

Full circles in Fig. 1 show τ_{e-e} versus the QW width for $f_i(\mathbf{k})$ taken as a constant distribution up to 36.8 meV above the AlGaAs barrier, which models the injected "barrier" distribution after a phonon cooling.[1,3] In the inset our calculation is compared with the result of Ref. 3. Both curves oscillate with the QW width and reach a resonant minimum, whenever a new bound state merges into the QW (the shift of our resonances to slightly lower QW widths is due to differ-

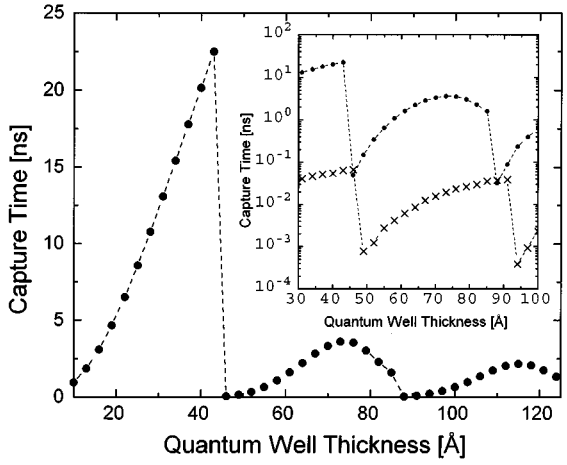

FIG. 1. E-e capture time τ_{e-e} vs the QW thickness for $N_S = 10^{11}$ cm^{-2}. In the inset these results are compared with the data (crosses) from Ref. 3.

ent effective masses in GaAs, AlGaAs and AlAs, which we considered when we calculated the electron wave functions). However, our τ_{e-e} is two-to-three orders larger. The difference of a factor of 4 is due to the missing factor of 1/4 in the e-e scattering rate of Ref. 3 (see Ref. 4 for details), but the remaining difference is still huge.

In order to provide insight we consider the QW width $w = 49$ Å. To demonstrate how the form factor [see Fig. 2(a)] affects the e-e scattering rate, we compare in Fig. 3(a) $\lambda_{ijmn}(g)$ as obtained using $F^2_{ijmn}(q)$, shown in Fig. 2(a), with $\lambda_{ijmn}(g)$ obtained with $F^2_{ijmn} = 1$. The latter is between $\sim 10^{12}$ s^{-1} and $\sim 4 \times 10^{12}$ s^{-1} for all capture transitions and its dependence on i,j,m,n is manifested through E_S. Figure 3(a) shows a quite different behavior and the relative importance of the individual transitions is determined by the form factors [Fig. 2(a)]. The individual capture times are at least

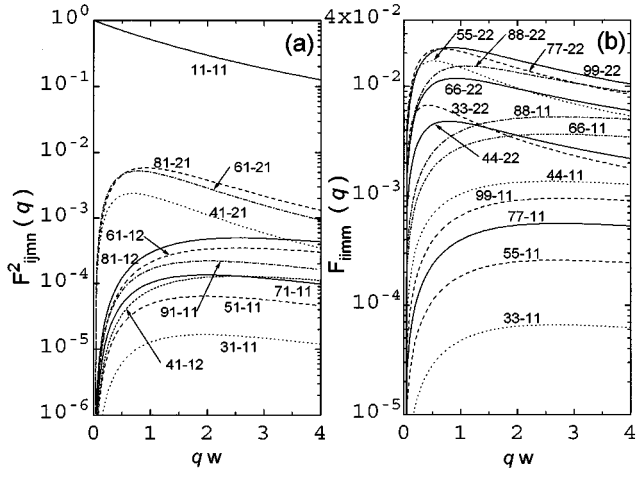

FIG. 2. (a) Square of the e-e scattering form factor $F_{ijmn}(q)$ vs the wave vector $\mathbf{q}$ for a QW with thickness $w = 49$ Å. The indices i,j and m,n label the initial and final states, respectively. States 1,2 are bound in the QW, states 3,4,...,9 have subband energies above the AlGaAs barrier. Except for the transition $11-11$ all other transitions are the e-e capture transitions. (b) The e-pop scattering form factors $F_{iimm}(q)$ are shown for comparison.

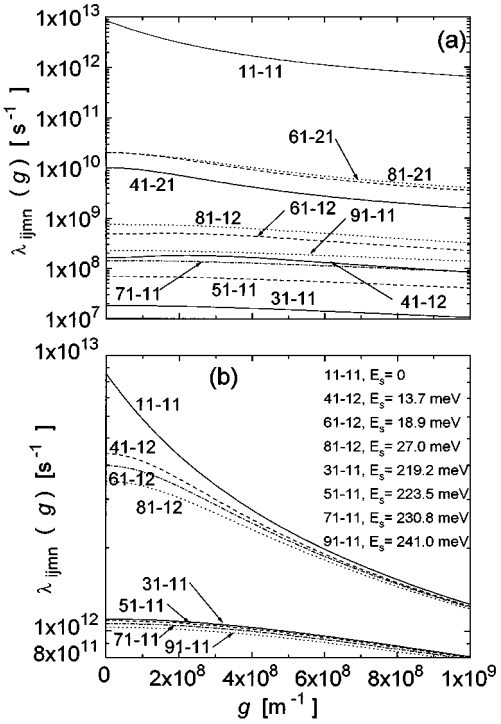

FIG. 3. E-e scattering rate λ_{ijmn} vs the wave vector $\mathbf{g}$. (a) Calculation with form factors from Fig. 2(a). (b) Calculation with $F_{ijmn} = 1$.

two orders larger than the subpicosecond capture times shown in Fig. 3(b). Subpicosecond e-e scattering is characteristic for intrasubband transitions as illustrated in Fig. 3 for $\lambda_{1111}(g)$. The form factor F_{1111} reduces $\lambda_{1111}(g)$ insignificantly and $\lambda_{1111}(g)$ values are close to similar calculations of Ref. 6. We believe that Ref. 3 predicts much smaller e-e capture times due to a numerical error. It is straightforward to verify Fig. 3(b) quantitatively, because formula (2) is reduced to a single-integral for $F_{ijmn} = 1$. As for the form factors, we can reproduce those published in Ref. 3. It can be seen that the results in Fig. 3(a) have correct order of magnitude, since they follow from Figs. 3(b) and 2(a).

The e-pop scattering rate of an electron with wave vector $\mathbf{k}$ from subband i to subband m reads (for emission)[7]

$$\lambda_{im}(\mathbf{k}) = \frac{e^2 \omega m^*}{8\pi\hbar^2}\left(\frac{1}{\kappa_\infty} - \frac{1}{\kappa}\right)\int_0^{2\pi} d\theta \frac{F_{iimm}(q)}{q\epsilon(q)}, \tag{5}$$

$$q = \left[2k^2 + \frac{2m^*}{\hbar^2}P - 2k\left(k^2 + \frac{2m^*}{\hbar^2}P\right)^{1/2}\cos\theta\right]^{1/2}, \tag{6}$$

where $P = E_i - E_m - \hbar\omega$, $\hbar\omega$ is the pop energy and κ_∞ is the high frequency permittivity. We calculate the e-pop scattering induced capture time τ_{e-pop} by averaging Eq. (5) as discussed for τ_{e-e}. Figure 4 compares τ_{e-pop} with τ_{e-e} parameters and the constant distribution $f_i(\mathbf{k})$ from Fig. 1. The τ_{e-pop} data shown by empty circles are calculated using the same static screening $\epsilon(q)$ as for the e-e scattering, empty squares show τ_{e-pop} for $\epsilon(q) = 1$. A calculation with dynamic screening will give results between these two extreme cases. We conclude that τ_{e-e} is one-to-three orders larger than τ_{e-pop} except for QW widths near the resonance

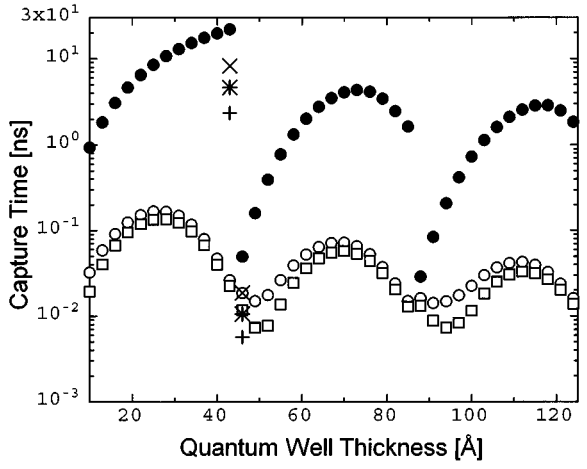

FIG. 4. E-pop capture time τ_{e-pop} and e-e capture time τ_{e-e} vs the QW thickness for $N_S=10^{11}$ cm^{-2}. Open circles show τ_{e-pop} for the statically screened e-pop interaction, open squares show τ_{e-pop} for the unscreened e-pop interaction and full circles are the τ_{e-e} data from Fig. 1. Crosses, asterisks and pluses at 43 Å and 46 Å show the τ_{e-e} data for $N_S=2.8\times10^{11}$ cm^{-2}, 5×10^{11} cm^{-2} and 10^{12} cm^{-2}, respectively.

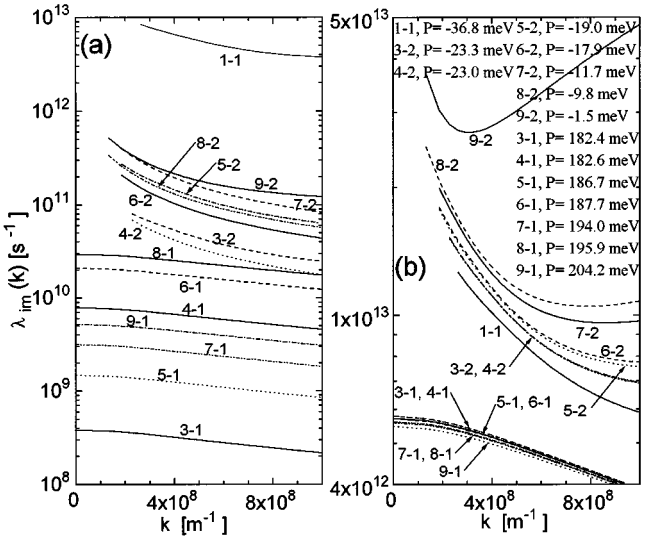

FIG. 5. E-pop scattering rate λ_{im} vs the wave vector $\mathbf{k}$ for the QW with width $w=49$ Å. (a) Calculation with form factors from Fig. 2(b). (b) Calculation with $F_{iimm}=1$.

minima. This conclusion differs from previous analysis[3] which predicts nearly the same oscillation amplitude in both cases. Reference 3 predicts that in the SCHQW lasers with a QW width below 40 Å the e-e capture causes significant excess carrier heating in the QW. Figure 4 does not support this conclusion, because the e-e capture is negligible.

Now we assess the dependence of both capture times on the electron density N_S. For $N_S\geqslant10^{11}$ cm^{-2} and temperature 8 K the static screening $\epsilon(q)$ is independent on N_S, because $f_1(0)\simeq1$. Therefore, the τ_{e-pop} values in Fig. 4 would be the same also for higher N_S and the τ_{e-e} values would decrease approximately like N_S^{-1} for each QW width. In Fig. 4 we show τ_{e-e} for $N_S=2.8\times10^{11}$ cm^{-2}, 5×10^{11} cm^{-2} and 10^{12} cm^{-2} at QW widths of 43 Å and 46 Å. At 43 Å τ_{e-e} is much larger than τ_{e-pop} even for $N_S=10^{12}$ cm^{-2} due to the absence of resonance. At 46 Å, when the first excited subband merges into the QW, τ_{e-e} resonantly decreases about 500 times and becomes smaller than τ_{e-pop} when $N_S\simeq5\times10^{11}$ cm^{-2}. When $N_S=10^{12}$ cm^{-2}, the total capture time $\tau_{e-e}\tau_{e-pop}/(\tau_{e-e}+\tau_{e-pop})$ is 3.8 ps for the unscreened e-pop capture ($\tau_{e-pop}=11$ ps) and 4.3 ps for the screened e-pop capture ($\tau_{e-pop}=18$ ps). Thus, compared to the case $\tau_{e-e}^{-1}=0$ the capture efficiency of the QW with the optimized (resonant) width can be improved with a factor 2.9−4.2 by increasing N_S to 10^{12} cm^{-2}. For $N_s>10^{12}$ cm^{-2} the capture time is expected to increase because the electrons interact with a coupled system of electrons and phonons.[8]

The τ_{e-pop} curve in Fig. 4 does not show a resonant drop for QW widths 46 Å and 88 Å, because the ''barrier'' electrons occupy the states below the threshold for pop emission and cannot be scattered into the subband which is in resonance with the top of the QW. A further increase of the QW width shifts the resonant subband deeper into the QW and the e-pop scattering into this subband smoothly increases. Figure 5 compares the unscreened e-pop scattering rates obtained using F_{iimm} from Fig. 2(b) with the rates obtained with $F_{iimm}=1$. The individual e-pop capture rates in Fig. 5(a) are governed by the relevant form factors, while for $F_{iimm}=1$ [Fig. 5(b)] one only finds a simple dependence on P. Compared to the e-e scattering rates in Fig. 3(a) the corresponding rates in Fig. 5(a) are systematically higher, because the e-pop capture rate Eq. (5) depends on F_{iimm} linearly while the e-e scattering rate Eq. (2) depends on F_{ijmn} quadratically. This fact makes the e-e capture less effective than the e-pop capture except for high electron densities.

In summary, the e-e and e-pop capture times in the SCHQW capture oscillate with the same period, but with very different amplitude. The e-e capture time is much larger than the e-pop capture time except for the QW widths near resonances, where it can be even smaller for electron densities close to 10^{12} cm^{-2} which leads to an improved capture efficiency of the QW. However, an inefficient e-pop capture in the SCHQW laser should not lead to excess carrier heating[4] due to e-e induced capture, because away from the resonance it is still much stronger than the e-e capture.

K.K. was supported by the Open Society Fund, Charta 77 Foundation and Slovak Grant Agency for Science, M.M. by the Slovak Grant Agency for Science, and F.P. by the Belgian National Science Foundation.

[1] J. A. Brum and G. Bastard, Phys. Rev. B **33**, 1420 (1986).
[2] P. W. M. Blom, C. Smit, J. E. M. Haverkort, and J. H. Wolter, Phys. Rev. B **47**, 2072 (1993).
[3] P. W. M. Blom, J. E. M. Haverkort, P. J. van Hall, and J. H. Wolter,, Appl. Phys. Lett. **62**, 1490 (1993).
[4] M. Moško, A. Mošková, and V. Cambel, Phys. Rev. B **51**, 16860 (1995).
[5] Ľ. Hrivnàk, Appl. Phys. Lett. **56**, 2425 (1990).
[6] M. Artaki and K. Hess, Phys. Rev. B **37**, 2933 (1988).
[7] A. Mošková, Ph.D. thesis, Comenius University, Bratislava (1992).
[8] P. Sotirelis and K. Hess, Phys. Rev. B **49**, 7543 (1994).